Electronic Research Archive

ERA, 31(9): 5685–5700.
DOI: 10.3934/era.2023288
Received: 30 June 2023
Revised: 01 August 2023
Accepted: 08 August 2023
Published: 16 August 2023

http://www.aimspress.com/journal/ERA

*Research article*

# Research on deformation prediction of deep foundation pit excavation based on GWO-ELM model

**Sanqiang Yang[1], Zhenyu Yang[1,*], Leifeng Zhang[1], Yapeng Guo[2], Ju Wang[2] and Jingyong Huang[3]**

[1] College of Civil Engineering and Architecture, Hebei University, Baoding, China
[2] Beijing Municipal Road and Bridge Co., LTD, Beijing, China
[3] Huitong Construction Group Co., LTD, Baoding, China

* **Correspondence:** Email: yzy32351@163.com.

**Abstract:** Given the complex nonlinear problem between the control and prediction of the surrounding surface settlement deformation caused (GWO), the GWO-ELM deep foundation pit excavation deformation prediction model was proposed. Extreme learning machine and Grey Wolf optimization algorithm combining training and predicting land subsidence. Based on MIDAS GTS NX software, we established a finite element simplified model for deep foundation pit construction, conducted structural calculations, and utilized the Grey Wolf optimization algorithm to optimize the deep foundation pit excavation and its influencing factors, input weights, and hidden layer thresholds in the ELM neural network. Taking the deep foundation pit project of Baoding Automobile Science and Technology Industrial Park as an example, the actual monitoring value is compared with the simulated value, verifying the model's accuracy. The number of soil nails in the finite element model, the excavation depth, the settlement of surrounding buildings and other factors are taken as the input factors of the prediction model. The DB-2 surface settlement of the monitoring point in the finite element model is taken as the output factor of the prediction model. The predicted value of the GWO-ELM model was compared with that of the ELM model. We draw three main conclusions from the results. First, the surface settlement of a bottomless foundation pit can be predicted in advance by using finite element software and the distribution law of surface settlement and horizontal displacement is consistent with the measured values. Second, the Grey Wolf optimization algorithm optimizes the input weights and thresholds in the extreme learning machine neural network. The GWO-ELM prediction model has good generalization ability, can effectively reduce human errors and can improve the accuracy of the prediction model. Third, through practical engineering verification, the average absolute error of the GWO-ELM model is 0.26145, the mean square error

is 0.31258 and the $R^2$ is 0.98725, all of which are superior to the ELM model and are an effective method for predicting deformation and settlement of deep foundation pit excavation.

**Key words:** deep foundation pit; neural network; Grey Wolf optimization algorithm; numerical simulation; extreme learning machine; prediction of settleme

## 1. Introduction

With the continuous development of our country's economy and society and continuous urban construction, above-ground resources can no longer meet people's needs and urban construction has gradually turned to underground development [1]. Underground engineering continues to expand in the direction of "*long, large and deep*", and the construction scale and difficulty of foundation pit engineering are increasing daily [2]. The construction of an urban foundation pit often has a complex surrounding environment and the excavation construction significantly impacts the surrounding environment [3]. Foundation pit engineering has the characteristics of solid regionalization and the monitoring and warning value varies significantly in different regions. For safe construction, it is significant to carry out construction control and deformation prediction for foundation pits [4–6].

In recent years, with the continuous development of computer science, finite element calculation and artificial neural networks have also been rapidly developed. They are widely used in the fields of mining and civil engineering. Machine learning is often used to predict flying rock distance and ground vibration during blasting, the ultimate bearing capacity of the single-driven pile and the performance of tunnel boring machines, etc. [7–10]. Armaghani et al. [11] used particle swarm optimization algorithm (PSO) -artificial neural network (ANN) and imperialist competitive algorithm (ICA)-artificial neural network and ordinary artificial neural network to predict the penetration rate of tunnel boring machine (TBM). It is found that ICA-ANN and PSO-ANN hybrid models are better than ordinary neural network prediction. With the continuous development of computer science, many advanced models are often used in time series prediction, such as ELM-PSOGWO, ANN-EMPA, LSTM-INFO, ELM-SAMOA, RVM-IMRFO [12–16]. Machine learning and optimization models have become powerful tools to approach and solve engineering problems due to the flexibility of technology. Because of the high complexity and nonlinearity of deep foundation pit excavation deformation prediction, a neural network is often used to research deep foundation pit excavation deformation prediction. Hong et al. [17] used convolutional neural networks and long short-term memory neural networks to integrate spatial features. They found that the accuracy and reliability of the combined model considering spatial-temporal correlation were higher than that of the LSTM model considering only temporal correlation. Niu et al. [18] adopted an ARIMA-NAR neural network combination model based on Kalman denoising for prediction analysis. Jiang et al. [19] proposed a (PSO-VMD)-NARX-GRU prediction model for landslide displacement, whose accuracy was significantly higher than that of BP, SVM and ARIMA prediction models in static models. Zhang et al. [20] optimized and modified the wavelet network model using weight parameters and gradient descent method and proved by engineering examples that the improved model could make the predicted value close to the measured value. Meng et al. [21] analyzed the horizontal displacement of containment through multi-step rolling prediction based on the BP neural network and found that the method was efficient and reliable. Based on the background of deep foundation pit engineering of a subway station in Suzhou, Zhao et al. [22]

adopted the 10-break cross-validation method based on the BP neural network and LSTM deep network to test the accuracy of the dynamic prediction model. They found that it has high reliability and generalization ability, which can provide a reference for construction information management.

In summary, many researchers have studied the deformation prediction method of deep foundation pits utilizing numerical simulation and machine learning neural networks. However, due to various errors, the prediction of environmental deformation around deep foundation pit excavation has certain limitations and the problems of large data dimension, slow model learning speed and low accuracy exist in the above prediction methods. This paper establishes a finite element simulation model based on engineering practice, the Grey Wolf optimization algorithm optimizes the extreme learning machine neural network and the GWO-ELM deep foundation pit excavation deformation prediction model is proposed. The ELM algorithm model is used to predict the excavation deformation of the foundation pit and the defects of slow learning speed and poor generalization performance of traditional neural networks are improved. GWO algorithm is used to optimize the ELM model to obtain the optimal input weight matrix and hidden layer deviation of the ELM algorithm, further improve the model's accuracy and provide specific theoretical reference and application value for the prediction of deep foundation pit engineering.

## 2. Project overview

### *2.1. Engineering background*

The research relies on the construction of a new rainwater and sewage pipeline laying project in Baoding Science and Technology Park. The size of the top pipe working well for the entire pipeline construction is a rectangular well with an internal clearance of 8.5 × 6 m and the receiving well is a rectangular well with an internal clearance of 5 × 5 m, with a depth of approximately 6.16–8.77 m. The foundation pit support is soil nail wall support and the safety level of the side of the foundation pit is Level 2.

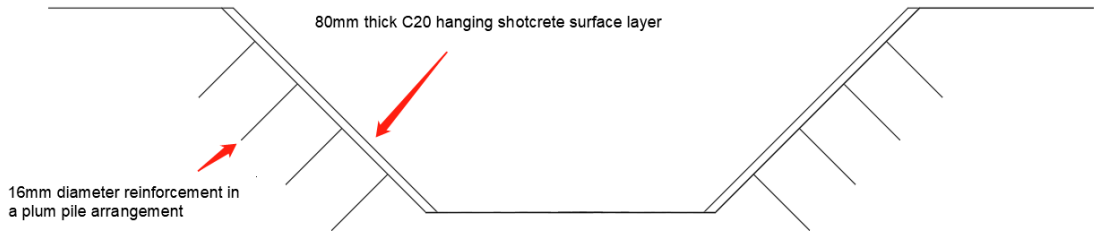


**Figure 1.** Sectional drawing of foundation pit support.

### *2.2. Geological conditions*

The soil layer parameter indicators and their distribution of this project are shown in Table 1.

**Table 1.** Soil layer parameter indicators and their distribution.

| Soil layer | Thickness/m | Unit weight of soil/ | Cohesion/kPa | Angle of internal |
|---|---|---|---|---|
| Plain fill | 0.30–1.00 | 18.8 | 17.5 | 22.9 |
| silt | 2.40–7.40 | 19.3 | 18.4 | 21.9 |
| Silty clay | 0.80–1.90 | 19.4 | 16.1 | 21.9 |
| silt | 1.00–2.50 | 19.6 | 19.4 | 21.7 |
| Fine sand | 2.00–7.80 | 19.5 | 17.2 | 21.1 |

### *2.3. Monitoring program*

The monitoring level of the foundation pit of this project is Level 1 and the soil nail support is Level 2. The impact of construction on the ground and underground pipelines, the safety of surrounding buildings, the stability monitoring of open caisson and the impact of construction on the stability of surrounding slopes are the key points of this monitoring plan. The specific monitoring point layout is shown in Figure 2.

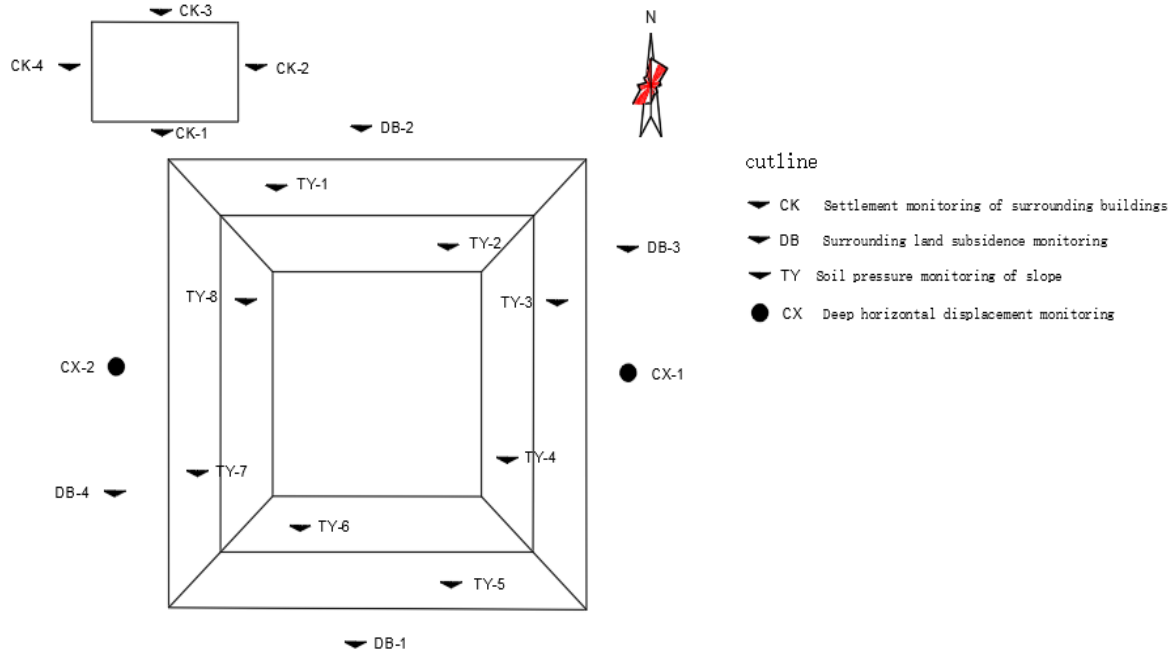


**Figure 2.** Layout of monitoring points.

## 3. GWO-ELM neural network model

### *3.1. Extreme learning machine model*

ELM is a new single hidden layer feedforward neural network algorithm [23–26]. Its biggest advantage is that the connection weights of the input layer and the hidden layer and the threshold of the hidden layer are randomly generated in the model training process. It does not need to be adjusted again after setting. It has the characteristics of simple structure and good generalization ability and has a fast rate.

Given a different training sample, $(x_i, t_i) \in R^n \times R^m (i = 1, 2, \ldots, N)$, SLFN output with $\tilde{N}$ hidden nodes is available.

$$o_j = \sum_{i=1}^{\tilde{N}} \beta_i f_i(x_j) = \sum_{i=1}^{\tilde{N}} \beta_i f(x_j; a_i, b_i) \quad j = 1, \ldots, N \tag{1}$$

where $o_j$ is the output of the network.

$a_i = [a_{i1}, a_{i2}, \ldots, a_{in}]^T$ and $b_i$ are the learning parameters randomly generated by the JTH hidden node, respectively. $\beta_i = [\beta_{i1}, \beta_{i2}, \ldots, \beta_{im}]^T$ is the output weight of the output node; $f(x_j; a_i, b_i)$ is the activation function of the original ELM. Let $a_i \cdot x_j$ be the inner product of $a_i$ and $x_j$. Equation (1) can be succinctly written as Eq (2).

$$H\beta = O \tag{2}$$

where:

$$H = \begin{pmatrix} f(a_1 \cdot x_1 + b_1) & \cdots & f(a_{\tilde{N}} \cdot x_1 + b_{\tilde{N}}) \\ \vdots & \ddots & \vdots \\ f(a_1 \cdot x_N + b_1) & \cdots & f(a_{\tilde{N}} \cdot x_N + b_{\tilde{N}}) \end{pmatrix}_{N \times \tilde{N}};$$

$$\beta = \begin{pmatrix} \beta_1^T \\ \vdots \\ \beta_{\tilde{N}}^T \end{pmatrix}_{\tilde{N} \times m} \quad ; \quad O = \begin{pmatrix} o_1^T \\ \vdots \\ o_N^T \end{pmatrix}_{N \times m};$$

where $H$ is the output matrix of hidden layer nodes; $\beta$ is the output weight; $O$ is the training set objective matrix.

$$\hat{\beta} = H^{+} T \tag{3}$$

Therefore, the three-step ELM algorithm can be summarized as follows.

Input: Training set $(x_i, t_i) \in R^n \times R^m (i = 1, 2, \ldots, N)$, activation function $f$, hidden node number $\tilde{N}$.

Output: Output weight $\beta$.

1) Randomly assign hidden node parameter $(a_i, b_i)$, $i = 1, \ldots, \tilde{N}$.

2) Calculate the output matrix of hidden layer $H$.

3) Calculate the output weight $\beta$, $\beta = H^{+}T$.

### *3.2. Grey Wolf optimization algorithm*

The GWO is a new meta heuristic algorithm with strong search capabilities proposed by Negi et al. [27]. This algorithm is based on the framework of systematization, recursive evolution and hierarchy. Due to its strong convergence performance and fewer parameters, its optimization performance is more reliable than other biomimetic algorithms [28–29].

The GWO optimization algorithm includes hunting and trapping of gray wolves and the hunting of prey is achieved through generation after generation. The main definitions of the algorithm are as follows:

a. The direct distance between the prey and the Wolf $\vec{D}$ is determined before the prey is eaten.

$$\vec{D} = \left| \vec{C} \cdot \vec{X}_P(t) - \vec{X}(t) \right| \tag{4}$$

where $t$ is the current number of iterations; $\vec{C}$ is the oscillation coefficient, $\vec{C} = 2\vec{r}_1$; $\vec{r}_1$ is the spatial distance coefficient $\vec{r}_1 = random(0,1)$; $\vec{X}_p(t)$ is the position vector of the t-generation gray wolf prey; $\vec{X}(t)$ is the current position vector of the t-generation gray wolf.

b. The position of the next generation of gray wolves is constantly updated to a shortened $\vec{D}$.

$$\vec{X}(t+1) = \vec{X}_p(t) - \vec{\mu} \cdot \vec{D} \tag{5}$$

$$\vec{\mu} = 2\vec{a} \cdot \vec{r}_2 - \vec{a} \tag{6}$$

where $\vec{X}(t+1)$ is the position vector of the t + 1 generation gray wolf; $\vec{\mu}$ is the coefficient; $\vec{r}_2$ is a random number of [0,1]; During the entire iteration process, $\vec{a}$ decreased from 2 to 0.

c. During predation, $\alpha$ wolves, $\beta$ wolves and $\delta$ wolves are closest to the prey. The distance between the other gray wolves of the t generation and these three wolves can be determined by the equation.

$$\vec{D}_k = \left| \vec{C}_i \cdot \vec{X}_k(t) - \vec{X}(t) \right| \tag{7}$$

$$\vec{X}_i = \vec{X}_k - \vec{\mu}_i \cdot \vec{D}_k \tag{8}$$

Predation direction is determined according to the following formula:

$$\vec{X}_p(t+1) = \frac{\vec{X}_1 + \vec{X}_2 + \vec{X}_3}{3} \tag{9}$$

where $k = \alpha, \beta, \delta$ and $i = 1,2,3$.

## 4. Engineering application

### *4.1. Finite element simulation*

Use MIDAS GTS NX software to establish a three-dimensional finite element calculation model for deep foundation pit excavation and analyze and study the surface deformation and settlement during the excavation process. The model size is the same as the physical engineering size, with a foundation pit side length of 18.5 m. According to engineering experience, the horizontal influence range is 4–6 times the physical engineering side length and the vertical influence range is 3–5 times the depth. The outer model has a side length of 60 m and a depth of 40 m. The foundation pit support adopts the method of spray anchor support. The boundary constraint adopts automatic constraints to constrain the translational degrees of freedom of the side and bottom nodes. Limit the horizontal displacement of the side, limit the horizontal displacement and normal displacement of the bottom.

The modified Moore-Coulomb model is selected as the soil constitutive model [30]. Compared with the ordinary Moore-Coulomb model, the simulated results of the modified Moore-Coulomb model are more appropriate to the unloading process of soil in deep foundation pit excavation. The results of model extraction are mainly concentrated in the vicinity of the foundation pit model, so the grid division of this part is relatively fine. The number of units in this calculation model is 12460 and the number of nodes is 10718. The model is shown in Figure 3.

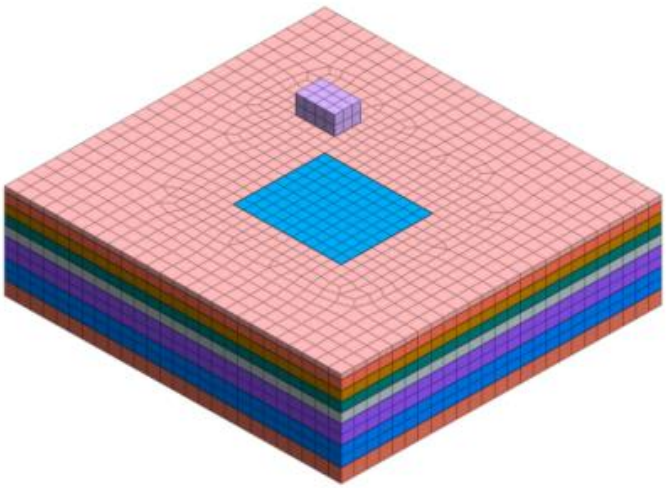

**Figure 3.** Excavation model of foundation pit.

Based on the excavation and support sequence at the construction site, the simulation of the foundation pit is divided into ten working conditions. Before excavation, balance the initial geostress and reset the displacement in the Z direction to zero.

Condition 1: Excavate the soil to –2 m.

Condition 2: Drive the first row of soil nails into the soil and spray concrete on the grid.

Condition 3: Excavate the soil to –4 m.

Working condition 4: Drive the second row of soil nails into the soil and spray concrete on the grid.

Working condition 5: Excavate the soil to –6 m.

Working condition 6: Drive the third row of soil nails into the soil and spray concrete on the grid.
Condition 7: Excavate the soil to a depth of –8 m.
Working condition 8: Drive the fourth row of soil nails into the soil and spray concrete on the grid.
Condition 9: Excavate to the bottom of the pit.
Working condition 10: Drive the fifth row of soil nails into the soil and spray concrete on the grid.

### *4.2. Settlement analysis of surrounding buildings*

Figure 4 Vertical displacement cloud map of some excavation conditions and Figure 5 contrast curve between measured and simulated settlement values of surrounding buildings.

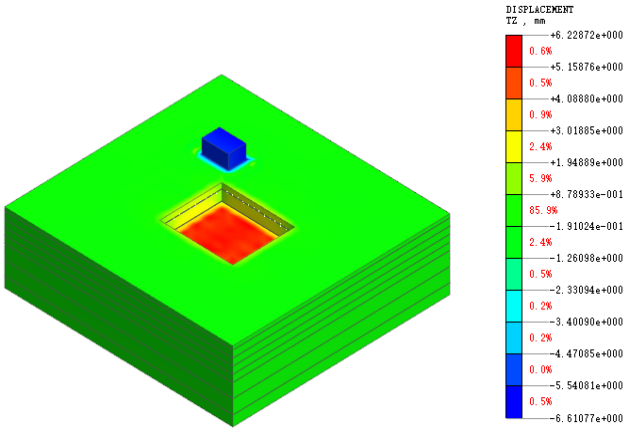


(a) Working condition one

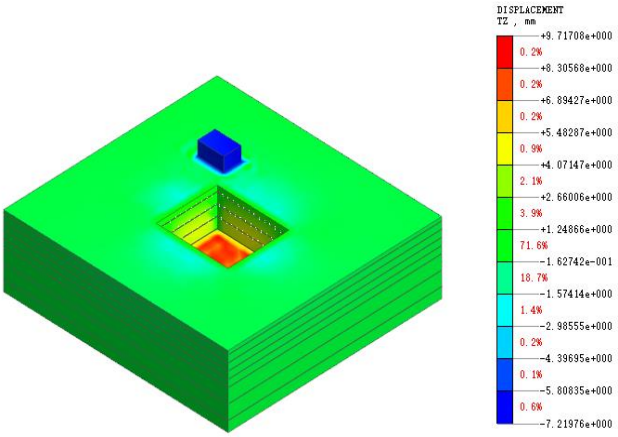


(b)Working condition five

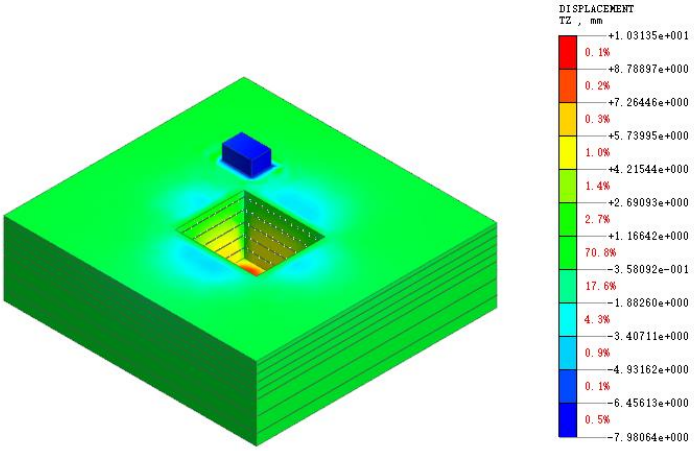


(c) Working condition nine

**Figure 4.** Simulation of vertical displacement of soil under various working conditions.

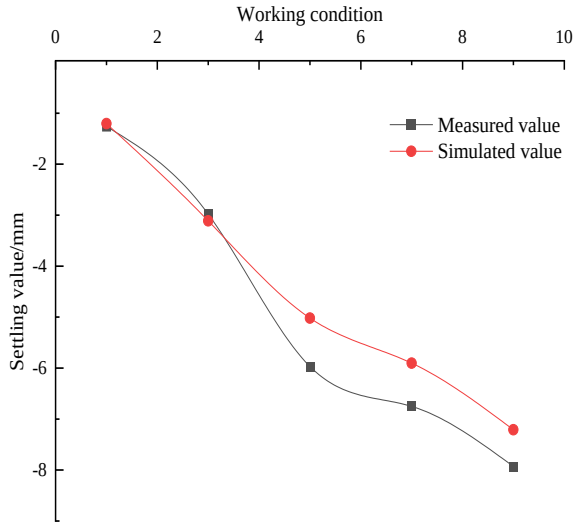


(a) Monitoring point CK-1

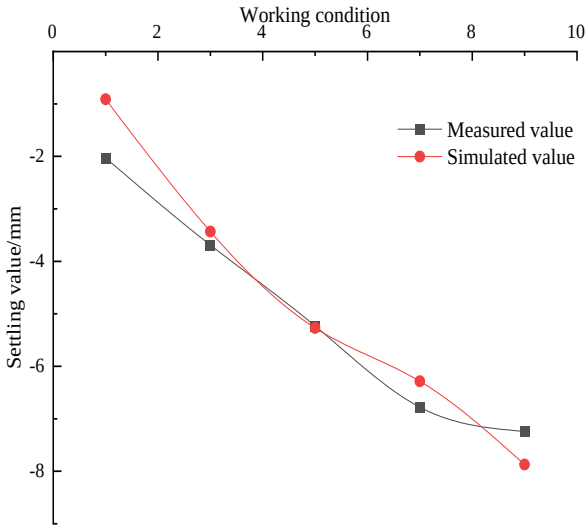


(b) Monitoring point CK-2

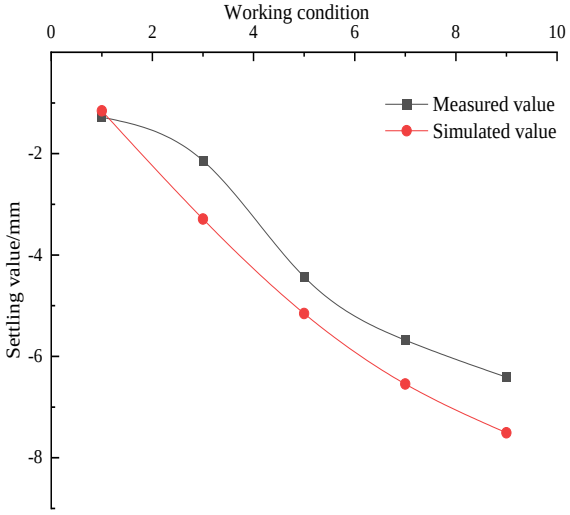


(c) Monitoring point CK-3

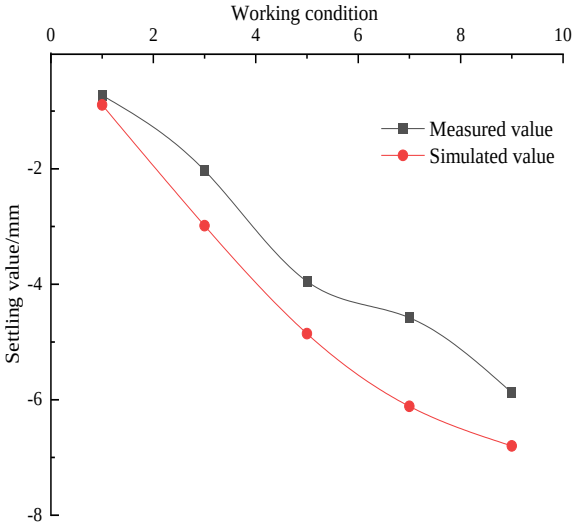


(d) Monitoring point CK-4

**Figure 5.** Comparison curve between measured and simulated settlement values at each monitoring point.

From Figures 4 and 5, it can be seen that as the construction progresses, the settlement of the garage on the northwest side of the foundation pit gradually increases. The shape of the actual value change curve is roughly the same as that of the simulated value change curve, but there is still a certain deviation. Overall, the simulated value is slightly larger than the measured value, which may be due to the software having a certain warning and protection effect. The measured value of monitoring point CK-1 is slightly greater than the simulated value because the monitoring point CK-1 is relatively close to the foundation pit and is greatly affected by the construction of the foundation pit. Some nearby loads and the impact of surrounding construction are not considered in the software. The maximum value monitored on site was 7.93 mm and the maximum value simulated by finite element analysis was 7.8709 mm, both of which did not exceed the warning value of 15 mm, indicating that the support structure was applied in a timely and effective manner.

### *4.3. Deep horizontal displacement analysis*

Figure 6 shows the cloud map of the deep horizontal displacement of the soil during the excavation of the foundation pit. Figure 7 shows the comparison curve between the monitoring values of the deep horizontal displacement of the soil after excavation and the finite element numerical simulation values.

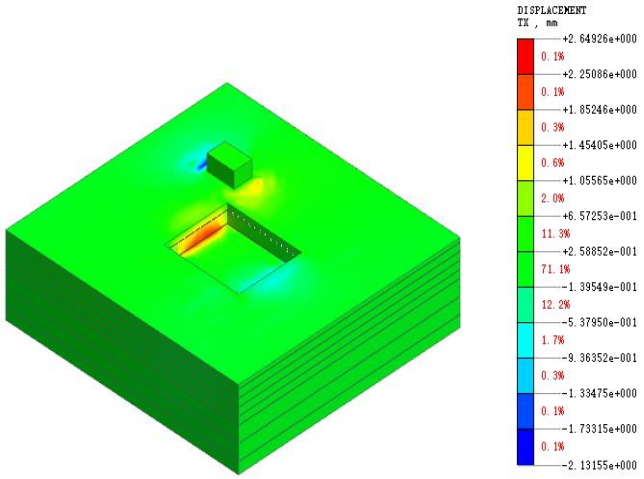


(a) Working condition one

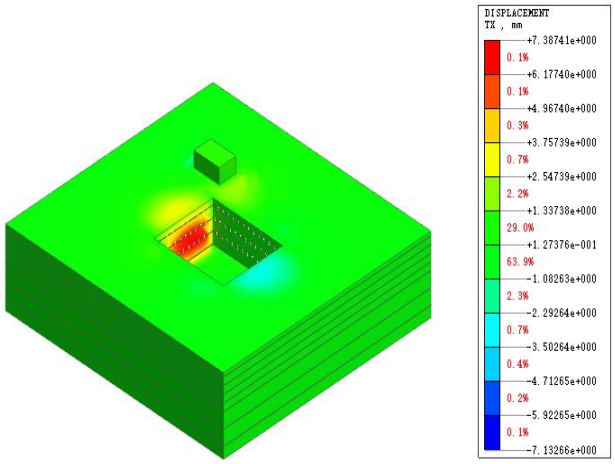


(b) Working condition five

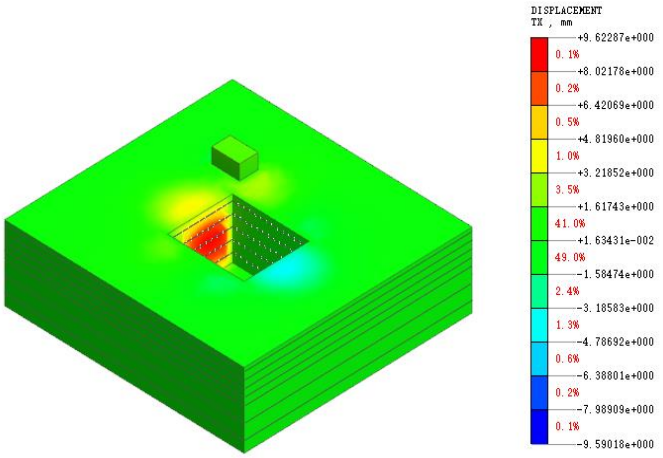


(c) Working condition five

**Figure 6.** Cloud map of deep horizontal displacement of foundation pit under different working conditions.

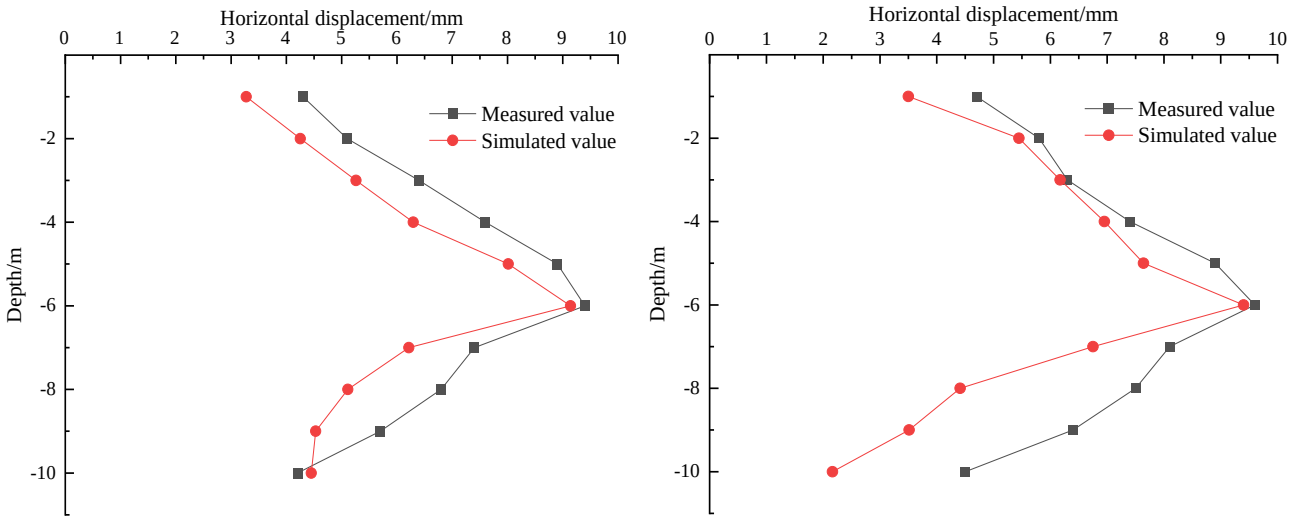


(a) Monitoring point CK-1

(b) Monitoring point CK-2

**Figure 7.** Comparison of measured and simulated horizontal displacement in deep foundation pit.

As can be seen from Figure 6, with the excavation of the foundation pit, each point on the side wall of the foundation pit moves toward the interior of the foundation pit and the horizontal displacement gradually increases. The horizontal displacement difference of each point in the same working condition does not exceed 10 mm. The maximum horizontal displacement of the side wall of the foundation pit is located in the middle of the slope. With the excavation of the foundation pit, the horizontal displacement reaches the maximum value. As can be seen from Figure 7, the overall trend of the measured horizontal displacement of deep foundation pit is roughly the same as that of the simulated value, which increases first and then decreases with the increase of the depth of foundation pit. However, there is still a deviation between the simulated value and the measured value and the maximum difference is 3.0887 mm. The simulated value is smaller than the measured value because mechanical vibration and vehicle flow are not taken into account in the simulation process.

To sum up, the measured value and the simulated value are compared and analyzed from two aspects: the settlement of surrounding buildings and the horizontal displacement in deep soil layer. From the results, there is still a certain error between the simulated value and the measured value, but the error is small. It can be used as the input data of the neural network.

### *4.4. Surface settlement prediction*

The monitoring point DB-2 in the north of the foundation pit was selected as the surface settlement prediction point, the excavation depth, the number of soil nails and the settlement of the building were taken as the input factors and the monitoring point DB-2 settlement value was taken as the output factors. The specific forecasting process is as follows:

(1) Weighted smoothing processing. In order to avoid the influence of accidental data on the prediction accuracy of the model, all the sample data are weighted with smooth noise reduction and balanced sample data.

(2) Data normalization processing. In order to eliminate the influence of different data dimensions, the prediction of excavation depth, number of soil nails and settlement value is normalized to the interval [0,1].

(3) Model parameter setting. The collected 60 data sets are sorted, the first 45 groups are selected as the training set, and the last 15 groups are selected as the test set. The network topology is $3 \times 20 \times 1$. The number of iterations is 1000 and the learning rate is 0.01. The depth of excavation, the number of soil nails and the settlement of the building are selected as the influencing factors, so the input layer node is set to 3. The model output is the surface settlement value, so the number of nodes in the output layer is set to 1. The number of neuron nodes in the hidden layer is set to 20. The Grey Wolf optimization algorithm optimizes the input weight and hidden layer threshold in ELM neural network. The size of the wolves is 40 and the number of iterations is 100. At the same time, the results are compared with those of the unoptimized ELM prediction model under the same conditions.

(4) Analysis of model prediction results. The predicted value of land surface settlement was obtained using the GWO-ELM prediction model and the test set results were shown in Table 2. The comparison diagram of DB-2 predicted value and error curve at monitoring points is shown in Figures 8 and 9. The prediction accuracy of different models is shown in Table 3.

**Table 2.** Neural network test set.

| Group number | Input factor Excavation depth/m | Number of soil nails/row | Building settlement/mm | Output factor Surface settlement value |
|---|---|---|---|---|
| 46 | 9 | 4 | 7.2653 | −7.195 |
| 47 | 9 | 4 | 7.4235 | –7.18 |
| 48 | 9 | 4 | 7.3598 | –7.18 |
| 49 | 10 | 4 | 7.5089 | –7.11 |
| 50 | 10 | 5 | 7.6214 | –7.11 |
| 51 | 10 | 5 | 7.5647 | –7.17 |
| 52 | 10 | 5 | 7.7851 | –7.17 |
| 53 | 10 | 5 | 7.6217 | –7.325 |
| 54 | 10 | 5 | 7.5236 | –7.325 |
| 55 | 10 | 5 | 7.6789 | –7.45 |
| 56 | 10 | 5 | 7.8452 | –7.45 |
| 57 | 10 | 5 | 7.8214 | –7.67 |
| 58 | 10 | 5 | 7.8687 | –7.67 |
| 59 | 10 | 5 | 7.7568 | –7.805 |
| 60 | 10 | 5 | 7.8951 | –7.805 |

**Table 3.** Precision comparison of models.

| Model name | Mean absolute error | Mean square error | $R^2$ |
|---|---|---|---|
| GWO-ELM | 0.26145 | 0.31258 | 0.98725 |
| ELM | 0.32412 | 0.45261 | 0.71243 |

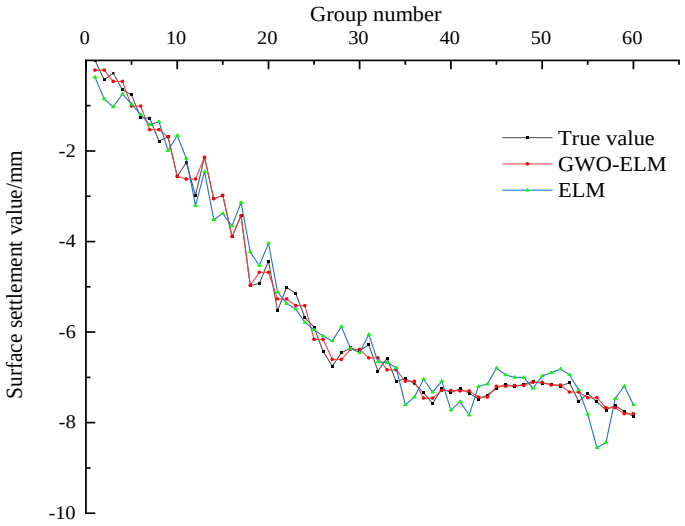


**Figure 8.** Comparison of DB-2 predicted values.

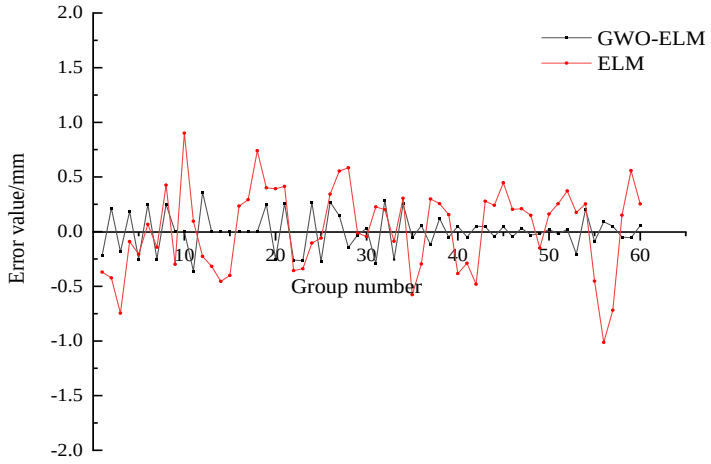


**Figure 9.** Comparison of error curves of DB-2 predicted value.

It can be seen from Figures 8 and 9 and Table 3 that the obtained root mean square error and average absolute error are 0.31258 and 0.26145, respectively, which are closer to the actual surface settlement and have smaller errors than the ELM prediction model. The determination coefficient $R^2 = 0.98725$ is higher than the ELM prediction model and the surface fitting effect is better, the prediction accuracy is higher and it has relative reliability.

## 5. Limitations and future works

The GWO-ELM and ELM prediction models adopted in this paper are used to predict the data in foundation pit excavation projects. These can provide a reference for the informatization construction of deep foundation pit excavation. Then, various unique data monitoring points can be further considered, monitored and predicted, such as vehicle load vibration, unpredicted rainfall and snow

amount of continuous rainfall and snowfall, earthquake impact, etc. This paper's monitoring and prediction project is based on the deep foundation pit project of Baoding Automobile Science and Technology Industrial Park. In the future, different foundation pit projects can be considered to be added or the engineering situation of all foundation pit projects in a particular area can be sorted out and the influencing factors and deformation causes of foundation pits can be comprehensively analyzed.

## 6. Conclusions

This article takes the excavation depth of the finite element model, the number of soil nails and the settlement of surrounding buildings as input factors and the surface settlement as output factors. Unlike using actual monitoring data as samples, it can achieve advanced prediction and is an effective analysis method.

The GWO-ELM based deformation prediction model for deep foundation pit construction excavation is significantly better than the ELM model and has achieved good prediction results. The model has good generalization ability and reduces human interference during the modeling process, making it an effective prediction method.

The mean absolute error of the extreme learning machine neural network optimized by gray wolf is 0.26145, the mean squared error is 0.31258 and the $R^2$ is 0.98725, which are better than the extreme learning machine neural network non-optimized.

## Use of AI tools declaration

The authors declare they have not used Artificial Intelligence (AI) tools in the creation of this article.

## Acknowledgments

This research was supported by the Natural Science Foundation of Hebei Province (E2018201106), the High-Level Talents Project of Hebei Province (B2017005024).

## Conflict of interest

The authors declare that there is no conflict of interest in the publication of this article.

## References

1. Y. Lv, T. Liu, J. Ma, S. Wei, C. Gao, Study on settlement prediction model of deep foundation pit in sand and pebble strata based on grey theory and BP neural network, *Arab. J. Geosci.*, **13** (2020), 1238. https://doi.org/10.1007/s12517-020-06232-7
2. H. Chen, J. Li, C. Yang, C. Feng, A theoretical study on ground surface settlement induced by a braced deep excavation, *Eur. J. Environ. Civ. Eng.*, **26** (2020), 1897–1916. https://doi.org/10.1080/19648189.2020.1739563
3. K. Chen, R. Xu, H. Ying, B. Li, X. Gan, Z. Pei, et al, Experimental study on excavation characteristics of a large 30.2m deep foundation pit in Hangzhou soft clay area, *Chin. J. Rock Mech. Eng.*, **40** (2021), 851–863. https://doi.org/10.13722/j.cnki.jrme.2020.0636

4. G. Zheng, Deformation control method and engineering application of foundation pit in Soft soil area, *Chin. J. Geotech. Eng.*, **44** (2022). https://doi.org/10.11779/CJGE202201001
5. X. Ni, C. Wang, D. Tang, J. Lu, X. Wang, W. Chen, Early warning and inducement analysis of super-large deformation of deep foundation pit in soft soil area, *J. Cent. South Univ.*, **53** (2022), 2245–2254. https://doi.org/10.11817/j.issn.1672-7207.2022.06.025
6. S. Qiao, Z. Cai, Z. Zhang, J. Tan, Characteristics of soft soil Long and narrow deep foundation pit retaining system in Nansha Port Area, *J. Zhejiang Univ. Eng. Sci.*, **56** (2022), 1473–1484. https://doi.org/10.3785/j.issn.1008-973X.2022.08.001
7. D. Armaghani, M. Hajihassani, E. Mohamad, A. Marto, S. Noorani, Blasting-induced flyrock and ground vibration prediction through an expert artificial neural network based on particle swarm optimization, *Arabian J. Geosci.*, **7** (2014), 5383–5396. https://doi.org/10.1007/s12517-013-1174-0
8. A. Dehghanbanadaki, M. Khari, S. T. Amiri, D. J. Armaghani, Estimation of ultimate bearing capacity of driven piles in c-phi soil using MLP-GWO and ANFIS-GWO models: a comparative study, *Soft Comput.*, **25** (2021), 4103–4119. https://doi.org/10.1007/s00500-020-05435-0
9. M. Khari, D. J. Armaghani, A. Dehghanbanadaki, Prediction of Lateral Deflection of Small-Scale Piles Using Hybrid PSO-ANN Model, *Arabian J. Sci. Eng.*, **45** (2020), 3499–3509. https://doi.org/10.1007/s13369-019-04134-9
10. C. Li, J. Zhou, M. Tao, K. Du, S. Wang, D. J. Armaghani, et al., Developing hybrid ELM-ALO, ELM-LSO and ELM-SOA models for predicting advance rate of TBM, *Transp. Geotech.*, **36** (2022), 100819. https://doi.org/10.1016/j.trgeo.2022.100819
11. D. Armaghani, E. Mohamad, M. Narayanasamy, N. Narita, S. Yagiz, Development of hybrid intelligent models for predicting TBM penetration rate in hard rock condition, *Tunn. Undergr. Sp. Tech.*, **63** (2017), 29–43. https://doi.org/10.1016/j.tust.2016.12.009
12. R. Adnan, R. Mostafa, O. Kisi, Z. Yaseen, S. Shahid, M. Zounemat-Kermani, Improving streamflow prediction using a new hybrid ELM model combined with hybrid particle swarm optimization and Grey Wolf optimization, *Knowl.-Based Syst.*, **230** (2021), 107379. https://doi.org/10.1016/j.knosys.2021.107379
13. R. Ikram, A. Ewees, K. Parmar, Z. Yaseen, S. Shahid, O. Kisi, The viability of extended marine predators algorithm-based artificial neural networks for streamflow prediction, *Appl. Soft. Comput.*, **131** (2022), 109739. https://doi.org/10.1016/j.asoc.2022.109739
14. R. Ikram, R. Mostafa, Z. Chen, K. Parmar, O. Kisi, M. Zounemat-Kermani, Water Temperature Prediction Using Improved Deep Learning Methods through Reptile Search Algorithm and Weighted Mean of Vectors Optimizer, *J. Mar. Sci. Eng.*, **11** (2023), 259. https://doi.org/10.3390/jmse11020259
15. R. M. Adnan, H. L. Dai, R. R. Mostafa, A. R. M. T. Islam, O. Kisi, A. Elbeltagi, et al, Application of novel binary optimized machine learning models for monthly streamflow prediction, *Appl. Water. Sci.*, **13** (2023), 110. https://doi.org/10.1007/s13201-023-01913-6
16. R. Adnan, R. Mostafa, H. Dai, S. Heddam, A. Kuriqi, O. Kisi, Pan evaporation estimation by relevance vector machine tuned with new metaheuristic algorithms using limited climatic data, *Eng. Appl. Comp. Fluid*, **17** (2023), 2192258. https://doi.org/10.1080/19942060.2023.2192258
17. Y. Hong, J. Qian, Y. Ye, Application of CNN-LSTM Model based on Spatial-temporal correlation characteristics in deformation prediction of foundation pit engineering, *Chin. J. Geotech. Eng.*, **43** (2021), 108–111. https://doi.org/10.11779/CJGE2021S2026

18. Q. Niu, Y. Li, M. Zhang, J. Fu, Y. Ma, Application of ARIMA-NAR neural network model based on Kalman filter in deep foundation pit settlement monitoring, *J. Lanzhou Univ. Technol.,* **48** (2022), 131–135.
19. Y. Jiang, W. Wang, L. Zou, R. Wang, S. Liu, X. Duan, Dynamic prediction model of landslide displacement based on particle swarm variational mode decomposition, nonlinear autoregressive neural network and gated cycle element, *Rock. Soil. Mech.*, **43** (2022), 601–612. https://doi.org/10.16285/j.rsm.2021.0247
20. B. Zhang, Y. Yao, J. Ji, Stochastic prediction of surface settlement of subway foundation pit based on wavelet neural network, *J. Railw. Sci. Eng.*, **18** (2021), 2899–2906. https://doi.org/10.19713/j.cnki.43-1423/u.t20210151
21. G. Meng, J. Liang, J. Huang, B. Wu, Q. Ou, Research on horizontal displacement prediction of deep foundation pit envelope based on BP artificial neural network, *Urban Rapid Rail Transit*, **35** (2022), 80–88.
22. H. Zhao, M. Zhang, W. Liu, P. Shi, Dynamic deformation prediction of deep foundation pit connecting wall based on neural network algorithm, *Chin. J. Undergr. Space Eng.*, **17** (2021), 321–327.
23. G. Huang, Q. Zhu, C. Siew, Extreme learning machine: Theory and applications, *Neurocomput.*, **70** (2006), 489–501. https://doi.org/10.1016/j.neucom.2005.12.126
24. S. Ding, X. Xu, R. Nie, Extreme learning machine and its applications, *Neural. Comput. Appl.*, **25** (2014), 549–556. https://doi.org/10.1007/s00521-013-1522-8
25. Z. Yaseen, R. Deo, A. Hilal, A. Abd, L. Bueno, S. Salcedo-Sanz, et al., Predicting compressive strength of lightweight foamed concrete using extreme learning machine model, *Adv. Eng. Softw.*, **115** (2018), 112–125. https://doi.org/10.1016/j.advengsoft.2017.09.004
26. M. Malekzadeh, S. Kardar, S. Shabanlou, Simulation of groundwater level using MODFLOW, extreme learning machine and Wavelet-Extreme Learning Machine models, *Groundwater Sustain. Dev.*, **9** (2019), 100279. https://doi.org/10.1016/j.gsd.2019.100279
27. G. Negi, A. Kumar, S. Pant, M. Ram, GWO: a review and applications, *Int. J. Syst. Assur. Eng. Manag.*, **12** (2021), 1–8. https://doi.org/10.1007/s13198-020-00995-8
28. Z. Guo, L. Chen, L. Gui, J. Du, K. Yin, H. Do, Landslide displacement prediction based on variational mode decomposition and WA-GWO-BP model, *Landslides*, **17** (2019), 567–583. https://doi.org/10.1007/s10346-019-01314-4
29. L. Zhang, X. Chen, Y. Zhang, F. Wu, F. Chen, W. Wang, et al., Application of GWO-ELM model to prediction of Caojiatuo landslide displacement in the three gorge reservoir area, *Water*, **12** (2020), 1860. https://doi.org/10.3390/w12071860
30. J. Bansal, S. Singh, A better exploration strategy in Grey Wolf optimizer, *J. Ambient Intell. Human. Comput.*, **12** (2021), 1099–1118. https://doi.org/10.1007/s12652-020-02153-1



AIMS Press